


Limit on the intergalactic magnetic field from the ultrahigh-energy cosmic ray hotspot in the Perseus-Pisces region

Andrii Neronov^{1,2}, Dmitri Semikoz¹, and Oleg Kalashev²

¹*APC, Université de Paris, CNRS, Astroparticule et Cosmologie, F-75006 Paris, France*

²*Laboratory of Astrophysics, Ecole Polytechnique Federale de Lausanne, 1015 Lausanne, Switzerland*

 (Received 20 December 2021; accepted 25 September 2023; published 8 November 2023)

The Telescope Array Collaboration has reported an evidence for existence of a source of ultrahigh-energy cosmic ray events in Perseus-Pisces supercluster. We show that the mere existence of such a source imposes an upper bound on the strength of intergalactic magnetic field (IGMF) in the Taurus void lying between the Perseus-Pisces supercluster and the Milky Way galaxy. This limit is at the level of 10^{-10} G for a field with correlation length larger than the distance of the supercluster (~ 70 Mpc). This bound is an order-of-magnitude stronger than the previously known bound on IGMF from radio Faraday rotation measurements and it is the first upper bound on magnetic field in the voids of the large-scale structure. Our analysis indicates that the source has to be dominated by protons, because heavier nuclei are either photodisintegrated or are too strongly deflected by the Galactic magnetic field.

DOI: [10.1103/PhysRevD.108.103008](https://doi.org/10.1103/PhysRevD.108.103008)

I. INTRODUCTION

The Telescope Array (TA) Collaboration has recently reported an evidence for existence of an excess of ultrahigh-energy cosmic ray (UHECR) events with energies above $E_{thr} = 2.5 \times 10^{19}$ eV in the direction $(RA, Dec) = (19^\circ, 35^\circ)$ of Perseus-Pisces supercluster [1,2]. The excess is observed at an angular scale $\Theta_{PP} = 20^\circ$, similar to the angular scale of excesses found earlier in combined HiRes/AGASA data with energies above 40 EeV [3], in the data of the Pierre Auger Observatory, near Cen A source [4] and in a previously reported “TA hotspot” [5] at the energy above 57 EeV. The new excess differs from the previously reported excesses in the sense that it has a well-identifiable counterpart, the Perseus-Pisces supercluster which is one of the largest and nearest mass concentrations in the local Universe, at the distance $D_{PP} \simeq 73$ Mpc, just behind the Taurus void of the large-scale structure [6,7].

UHECR mass composition studies show that the fraction of heavy nuclei in UHECR flux increases at high energies [8,9]. Modeling of propagation of heavy nuclei through the intergalactic medium and through the galactic magnetic field (GMF) suffer from large uncertainties that complicate interpretation of the UHECR data on previously known excesses. The newly found TA excess [1,2] is at lower energies and potentially can contain larger fraction of protons and helium that are easier to trace from the source to the Earth.

Trajectories of UHECRs are affected by magnetic fields in the host galaxy, galaxy cluster or supercluster, in the intergalactic medium and finally in the Milky Way galaxy. Constrained simulations of magnetic field in the large-scale

structure in nearby 100 Mpc and its influence on UHECRs was first studied in Ref. [10] and later independently in Ref. [11]. In both cases deflection of cosmic rays was found to be dominated by the fields in the filaments of the large-scale structure. A strong enough magnetic field in the source located in a galaxy cluster or supercluster may randomize the directions of UHECR particles in an energy-dependent way and change the observational appearance of a source and its spectrum [12]. The Perseus-Pisces supercluster, the suggested source of UHECR, spans a $>40^\circ$ long filament aligned with the Galactic latitude direction [6] in the outer Galaxy part of the sky. The strong magnetic field in the supercluster may well spread UHECRs across this large region and explain the extension of the TA source.

A magnetic field in the Milky Way has a different effect on the observational appearance of the source. Its regular component displaces the source from its reference position on the sky [13], while its turbulent component broadens the source extent [14]. This broadening is at maximum 7° , which is moderate compared to the observed source extent [14]. Contrary to the turbulent field, the displacement by the regular GMF is estimated to be sizeable in the energy range of interest [13], $\Theta_{gal} \simeq 15^\circ Z [E/E_{thr}]^{-1}$ where Z is the atomic number of the UHECR nuclei. It is comparable with the extent of the Perseus-Pisces supercluster on the sky and to the observed angular extent of the UHECR source.

Contrary to the GMF, presence of the intergalactic magnetic field (IGMF) between the source and the Milky Way galaxy can potentially not only transform the source appearance, but completely wash out the UHECR source from the sky. The mere existence of an isolated

UHECR source thus limits the IGMF strength. In what follows, we use this fact to derive, for the first time, an upper bound on IGMF in a void of the large-scale structure.

II. UHECR BACKTRACING METHOD

This section provides a description of our simulations setup and numerical techniques for the UHECR backtracing through the Galactic magnetic field.

Propagation of cosmic rays from extragalactic sources can be divided into several stages. First, they have to escape from the local environment of the UHECR source. Then they travel through the intergalactic medium filled with the magnetic field that we aim to constrain, and finally they pass through the Milky Way galaxy to reach the observer.

Propagation inside the UHECR source influences anisotropy and spatial pattern of emission from the source. We do not model the intrinsic source properties, because the quality of the UHECR data is not sufficient for such studies. The source may well be almost point source at the location of Perseus cluster or an extended source spanning all the Perseus-Pisces supercluster. The details of the source morphology do not change our conclusions. For propagation through the Taurus void, we use analytical formulas for a homogeneous or tangled magnetic field, which are robust in the sense that they are model independent. Model-dependent tighter bounds may be derived if details of the large-scale structure along the line-of-sight is taken into account e.g., based on “constrained” simulations like the recent Sibelius simulation [15], but such model-dependent study is beyond scope of our paper.

We model propagation of UHECR through the Galactic magnetic field of the Milky Way via backtracing of UHECR in a galactic magnetic field. We make the code for such backtracing publicly available via the link [16]. We have cross-checked the results based on this code with similar backtracing code implemented in the CRPropa cosmic-ray propagation library [17]. Both codes provide the possibility to follow charged particle trajectories in a predefined three-dimensional magnetic field, which can include both regular and turbulent components. To reliably determine the pattern of arrival directions of UHECR, we backtrace trajectories of 2×10^4 UHECR particles with energies $E = E_{thr} = 10^{19.4}$ eV and (alternatively) 2×10^4 UHECR with energies above the energy E_{thr} distributed according the spectrum of UHECR measured by the Telescope Array experiment. We repeat simulations for different particle types; protons, helium, and carbon. We have checked that both approaches (fixed energy and energies distributed according to the measured UHECR spectrum) give practically same results. We have also checked that increasing of number of backtraced particles does not affect our final results.

We use the regular magnetic field model of Ref. [13] and compare the results with alternative models of Refs. [18–22]. The large-scale random (striated) field

and a small-scale random (turbulent) magnetic field component is provided only for Jansson-Farrar model [19] and its improved variants from Refs. [21] and [22].

Our backtracing code and CRpropa differ in their treatment of the turbulent magnetic field. In CRPropa the turbulent field parameters are derived from the publication [13]. In our code we take into account a correction that considers the fact that the original Jansson-Farrar turbulent field is too high and it would prevent low-energy cosmic rays to escape from Galaxy, thus contradicting the observations of primary-to-secondary cosmic-ray nuclei ratios [23].

The parameters of the turbulent component of the Galactic magnetic field are largely uncertain. Dependence of a UHECR deflection pattern on coherence length of magnetic field with our code was studied in Ref. [24]. In more general settings, the uncertainty of the ratio of the regular and turbulent magnetic field strengths and their relation to the escape of cosmic rays of different energies and to the measurements of secondary nuclei was studied with our code in Ref. [25].

III. ESTIMATE OF THE EFFECT OF THE GMF

Our knowledge of geometry of the GMF suffers from large uncertainties, see [26] for a review and a detailed discussion. This geometry has been inferred from the data on the Faraday rotation measure of pulsars [27] and extragalactic sources [28] that provide information on the integral of projected magnetic field strength along different sky directions, weighted with the density of free electrons in the interstellar medium. Uncertainties of the distribution of the free electrons induce large systematic errors in the modeling. Account of the data on synchrotron emission from the interstellar medium provides information on the total strength of the field, but introduces an additional dependence of the result on the uncertain distribution of cosmic ray electrons.

The systematic uncertainty of the GMF modeling may be estimated from comparison of different models that derive quite different overall field geometries [13,20,26]. To assess this uncertainty, we compare predictions of different models for the source position on the sky. The result of backtracing of UHECR trajectories through the regular component of the GMF is shown in Fig. 1. The green region shows the source location on the sky, as reported by the TA experiment (a 20° radius circle, shown in Galactic coordinates, Aitoff projection centered at the Galactic anticenter). Left panel of the figure shows the result of backtracing of the source circle through the GMF into the intergalactic space for proton UHECRs. Red, white, and cyan contours shows the backtraced cones for different GMF models of Refs. [13,18,20]. One can see that the models agree in the general trend, deformation, and shift of the circular region closer to the Galactic plane, produced by specific direction of the ordered GMF in the outer galaxy. However, the models strongly disagree in the region close to zero Galactic latitude.

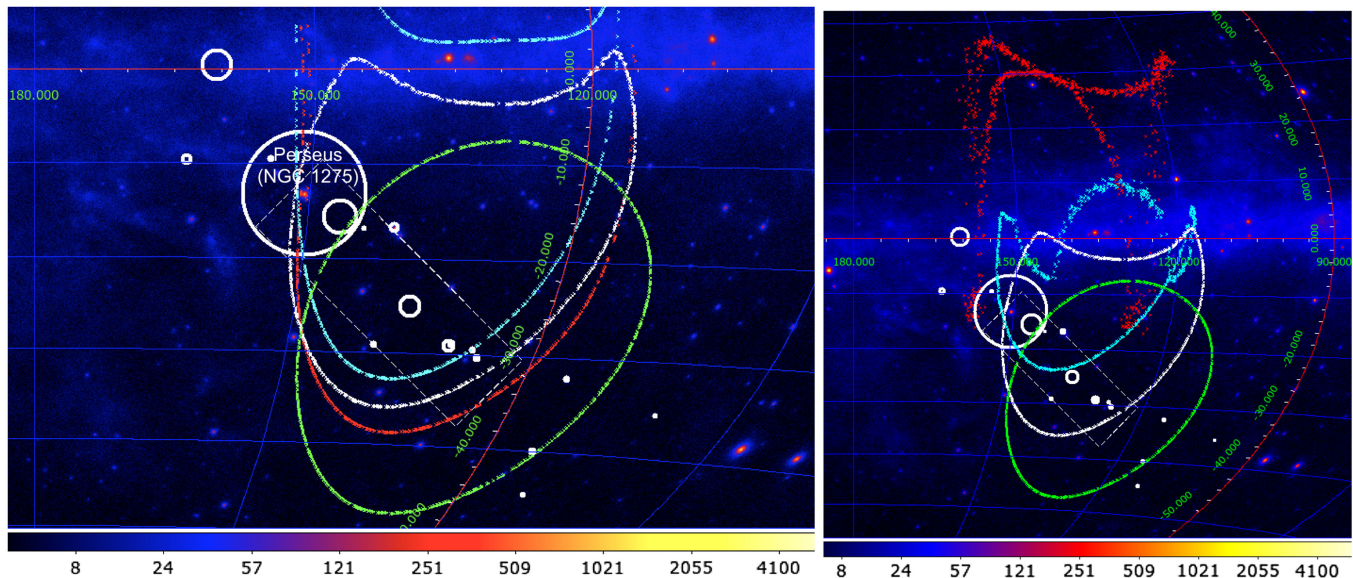


FIG. 1. Left: UHECR source location chart on top of the Fermi/LAT count map of γ -ray events with energies above 1 GeV. Green region shows the location and extent of the UHECR source of TA. Color contours show respectively the backtracing of the source circular region through the GMF in different models; red for the model of Ref. [13], white for the model of Ref. [18], cyan for that of Ref. [20]. White circles show the locations of largest galaxy clusters and groups in Perseus-Pisces supercluster [7]. Size of the circles is proportional to the mass of the object. The dashed rectangle of the size $30^\circ \times 10^\circ$ shows the direction of filamentary alignment of the supercluster components within the extent of the backtraced UHECR source. Right: same as the left panel, but the contours shown are the original UHECR source (green) and the backtracing of the source through the GMF model of Ref. [13] assuming that the UHECR are protons (white), helium (cyan), or carbon (red) nuclei. The energy of UHECR particles is 2.5×10^{19} eV.

The models of [18,20] predict that part of the signal may be coming from the positive Galactic latitude region, not at all from the direction of the Perseus-Pisces supercluster. This large discrepancy between the model predictions is related to the larger uncertainty of the detailed structure of magnetic field at (multi)kiloparsec distances along the Galactic disk. To the contrary, the agreement between the models is better in the higher negative Galactic latitude region, where only better constrained GMF in the local interstellar medium influences UHECRs.

Turbulent component of the GMF can be taken into account for the Jansson-Farrar model [13,19]. We checked that in original version of this model smearing of cosmic rays by turbulent field is below 3 degrees at 25 EeV. However the turbulent component in Jansson-Farrar model perhaps still an overestimate; such strong turbulent field reduces the escape rate of low-energy cosmic rays and increases the boron-to-carbon ratio of the cosmic rays flux beyond the observed value, as was shown in [24].

IV. UHECR FROM SOURCE(S) IN PERSEUS-PISCES SUPERCLUSTER

A. Possible primary UHECR source(s) in Perseus-Pisces supercluster

White circles in Fig. 1 show locations of the largest galaxy clusters and groups in the Perseus-Pisces supercluster. Overall, this nearby mass concentration appears

filamentlike on the sky [6] and the filament direction (outlined by the dashed box) can be inferred from the alignment of the largest mass concentrations, visible in the figure (from [7]). The dominant mass concentration is by far the Perseus cluster. Its location is not within the extent of the UHECR source detected by the TA, but it enters the source extent once the source cone is backtraced through the GMF. This result does not depend on the choice of the GMF model. The Perseus cluster hosts several TeV γ -ray emitting active galactic nuclei (AGN) (NGC 1275, IC 310) [29,30]. UHECR acceleration and interactions are expected to be associated with the TeV γ -ray emission [31], and hence these γ -ray sources in the Perseus cluster may be the points of initial injection of UHECR in Perseus-Pisces supercluster. Improving quality of UHECR data with TAX4 experiment [32] may be needed to verify this hypothesis and distinguish it from alternative possibilities, like injection from a large number of star-forming and star-burst galaxies distributed over the super-cluster volume.

B. Propagation of UHECR from source

The Perseus-Pisces supercluster is located at a distance 70 Mpc from us and UHECRs lose energy on their way to Milky Way. We have estimated the effect of photodisintegration on the atomic nuclei in the UHECR flux. The result is shown in Fig. 2. We assume that spectrum of source located in Perseus-Pisces supercluster is $1/E^2$ up to

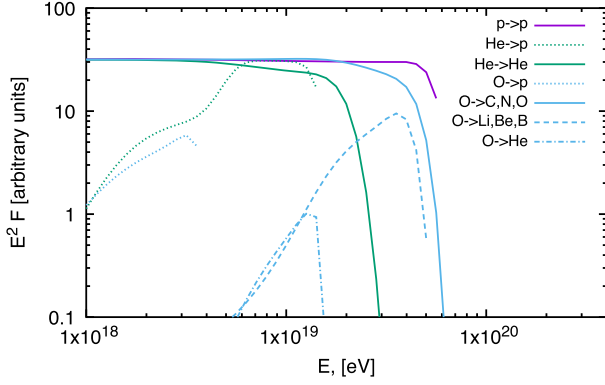


FIG. 2. Spectrum of protons, He and CNO nuclei after a propagation of distance 70 Mpc from the Perseus-Pisces supercluster to Milky Way.

$E_{\max} = 10^{20}$ eV. The attenuated spectrum of protons is shown with violet line. The He spectrum is shown with green line. One can see that He nuclei with energies $E_{th} > 2.5 \times 10^{19}$ eV can not reach us from the source distance. Contrary to He, CNO nuclei still can reach us. In particular O can be transferred to N or C by photodisintegration reactions, but still large number of CNO still come at $E_{th} > 2.5 \times 10^{19}$ eV. Thus, the spectrum of the source Perseus-Pisces supercluster reach the Milky Way at $E_{th} > 2.5 \times 10^{19}$ eV and can be dominated by protons or CNO nuclei, but not by He.

C. Constraints on mass composition of the UHECR source form the source geometry

The right panel of Fig. 1 shows the result of backtracing of the source circle through the GMF of Ref. [13] for different atomic nuclei. Increase of the atomic number Z leads to larger displacement of the backtraced region toward the Galactic plane. The backtraced region still covers part of the extent of the Perseus-Pisces supercluster in the case of $Z = 2$ (helium nuclei), but it is completely displaced to the positive Galactic latitude for $Z = 6$ (carbon). This suggests that the UHECR source flux has to be dominated by protons, since He can not come from 70 Mpc away source, and CNO dominated source would be too strongly displaced. A source produced by protons coming directly from the direction of Perseus cluster is generically expected to have an extent of $\gtrsim 30$ degrees at the energy $E \gtrsim 2.5 \times 10^{19}$ eV, because of the energy dependence of the UHECR deflection angle.

V. A LIMIT ON THE INTERGALACTIC MAGNETIC FIELD

As is mentioned in the Introduction, the mere existence of an individually detectable UHECR source (be it the

Perseus cluster, or the entire filamentlike Perseus-Pisces supercluster) indicates that the IGMF is not strong enough to “erase” the source from the sky. Homogeneous IGMF of the strength B deflects the UHECR particles by an angle [33] $\Theta \simeq 15^\circ Z [E/E_{thr}]^{-1} [B/10^{-10} \text{ G}] [D/70 \text{ Mpc}]$. A regular IGMF as strong as $B \sim 10^{-9}$ G all over the distance $D \sim D_{PP} \simeq 70$ Mpc toward the source would deviate UHECRs by hundred(s) of degrees so that they would not even be able to reach the Milky Way. Thus, the source extent of $\Theta_{\text{UHECR}} = 20^\circ$ imposes a limit on the homogeneous IGMF at the level of

$$B \leq 1.3 \times 10^{-10} Z^{-1} \left[\frac{\Theta}{\Theta_{\text{UHECR}}} \right] \left[\frac{D}{D_{PP}} \right]^{-1} \left[\frac{E}{E_{thr}} \right] \text{ G}. \quad (1)$$

The uncertainty of the composition of UHECR flux does not allow to determine the characteristic atomic number of events contributing to the signal, so the conservative assumption is $Z = 1$. This limit is shown as the horizontal lower boundary of the red-shaded region in Fig. 3.

IGMF homogeneous on the distance scale comparable to the distance to the Perseus-Pisces cluster can only originate from the epoch of inflation in the early Universe (see e.g., [41]). All other physical mechanisms of magnetic field generation (cosmological phase transitions or magnetized outflows from galaxies) result in the fields with much shorter correlation length; [36] $\lambda_B \simeq 1 [B/10^{-8} \text{ G}] \text{ Mpc}$ for the phase transition field, $\lambda_B \sim 10\text{--}100 \text{ kpc}$ for the outflows. In this case, $\lambda_B \ll D_{PP}$ and the deflection angle of UHECR is estimated as [33] $\Theta \simeq 15^\circ [E/E_{thr}]^{-1} [B/10^{-10} \text{ G}] [D/70 \text{ Mpc}]^{1/2} [\lambda_B/70 \text{ Mpc}]^{1/2}$. The constraint $\Theta < \Theta_{\text{UHECR}}$ imposes a restriction $B < 1.3 \times 10^{-10} [\lambda_B/70 \text{ Mpc}]^{-1/2} \text{ G}$. This limit is shown as an inclined boundary of the red-shaded region in Fig. 3. For the larger coherence length (comparable or larger than the distance to the source), the exact value of the bound in Fig. 3 depends on the angle between ordered fields in the void. The value shown in Fig. 3 is angle averaged.

VI. DISCUSSION

Detection of a UHECR source in the direction of Perseus-Pisces cluster [1] implies an upper bound on IGMF at the level shown by the red-shaded range in Fig. 3. This bound is an order-of-magnitude tighter than the bound from non-observation of excess Faraday rotation signal in the polarized radio fluxes from extragalactic sources [37,42]. Moreover, this is the bound on a different kind of IGMF. The UHECR deflections are proportional to the integral of the magnetic field component orthogonal to the line-of-sight; $\Theta_{\text{IGMF}} \propto \int_{los} B_\perp dl$. To the contrary, the Faraday rotation measure depends on the line-of-sight integral of the parallel magnetic field weighted with the free-electron density n_e ; $RM \propto \int_{los} B_\parallel n_e dl$. The rotation measure bound

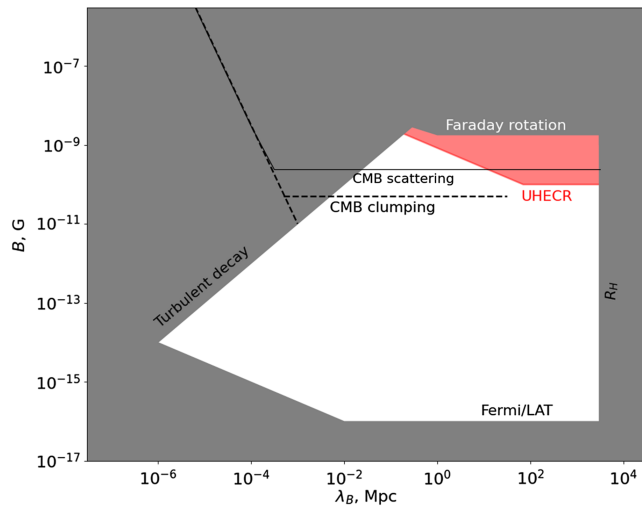


FIG. 3. Previously known bounds on the present-day IGMF strength and correlation length (gray) compared to the UHECR bound derived in the text (red). Lower bound from γ -ray observations, marked “Fermi/LAT” is from [34,35]. The bound marked “Turbulent decay” corresponds to the size of largest turbulent eddies that can be processed on cosmological timescale [36]. The bound marked “ R_H ” corresponds to the Hubble distance scale. The bound from the Faraday rotation is from [37,38]. Dashed and solid black lines show constraints on comoving cosmological field strength 3×10^5 yr after the Big Bang, derived in Refs. [39] (“CMB scattering”) and [40] (“CMB clumping”).

rather constrains the magnetic fields in the high n_e regions, namely in halos around galaxies and galaxy clusters. To the contrary, UHECR deflections probe the average field along the line-of-sight toward UHECR source.

The lines-of-sight toward the Perseus-Pisces supercluster or toward the Perseus cluster both pass through the well-known Taurus void [6] (in fact, the Perseus-Pisces supercluster is the boundary of this void, while the mass concentration hosting the Milky Way is the boundary on the other side of the void). Thus, the limit presented above constrains the magnetic field strength in the Taurus void. This is the first time when an upper bound on the void magnetic field is reported.

Our analysis shows that the UHECR excess in the direction of Perseus-Pisces cluster [1] should be dominated by protons. Indeed, the right panel of Fig. 1 shows that only deflections of protons or He nuclei by the Galactic magnetic field are small enough to remain in the Perseus-Pisces sky region. At the same time, Fig. 2 shows that He nuclei can not reach us from the 70 Mpc distance. Thus, only protons can contribute to the excess of UHECR from the source.

The lower bound on the magnetic field in the voids is imposed by nonobservation of secondary extended and delayed γ -ray emission around high-energy γ -ray loud AGN [33,43,44]. This bound is currently at approximately 10^{-16} G for the large correlation-length magnetic

fields [34,35], see Fig. 3. Thus, a combination of this lower bound with the new upper bound from UHECR observations provides the first measurement of the void IGMF 10^{-16} G $< B < 10^{-10}$ G. Measurements of the void IGMF will be improved in the future by the CTA telescope [45] that will be able to measure the magnetic field up to 10^{-11} G [46]. Together with possible improvement of UHECR observations this can shrink the uncertainty of the void IGMF strength to less than an order of magnitude.

The void magnetic fields are most probably of cosmological origin [41,47,48]. However, before this can be stated with certainty, one has to verify if the voids are not “polluted” with magnetic fields spread by galactic outflows [49]. State-of-art modeling of star formation and AGN driven magnetized outflows from galaxies [50–52] shows that these outflows most probably are not strong enough to fill the voids.

If the void fields are of cosmological origin, the UHECR bound on the field in the Taurus void may be compared to the bounds from the cosmological tracers of the magnetic field. Presence of magnetic fields during the recombination epoch induces small-scale clumping of baryonic matter and modifies the recombination dynamics [40]. Nonobservation of this effect imposes a bound on cosmological field at the level of the dashed lines in Fig. 3. The magnetic field also induces distortions to the matter power spectrum that affect the process of formation of dwarf galaxies [53]. This, in turn, leads to earlier formation of the first stars and modification of dynamics of the reionization. Nonobservation of excess scattering of the CMB photons by free electrons generated by early reionization [39] imposes a bound on the cosmological IGMF at the level of the solid lines in Fig. 3.

The UHECR bound on the large correlation length cosmological magnetic field (that would originate from inflation) is stronger than the Faraday rotation [37,38] and CMB bounds [54,55] and is somewhat stronger than the limit from nonobservation of magnetic field-induced excess optical depth of the CMB signal [39] and is somewhat weaker than the limit imposed by the nonobservation of faster recombination [40]. Closeness of the bounds from three different techniques indicates that improvement of the sensitivity of these techniques may result in a “multi-messenger” detection of an inflationary cosmological magnetic field, if it has scale-invariant power spectrum and a field strength close to $B \sim 10^{-10}$ G.

The bound on IGMF derived in this paper is comparable to previously reported constraints from the observational evidence of correlation of UHECR arrival directions with candidate UHECR source classes [56,57], such as star-forming galaxies [58]. This previous analysis suffers from much larger uncertainties, compared to our analysis.

The analysis of correlation of UHECR arrival directions with entire source populations is affected by the systematic uncertainty of the deflections of UHECR by the GMF discussed above (see Fig. 1), as well as the uncertainty of distances to the UHECR sources contributing to the correlation. The analysis of source populations also does not allow us to constrain the magnetic field in the voids of the large-scale structure; the lines of sight to different sources forming a population may pass through voids, filaments, sheets or even highly magnetized halos.

ACKNOWLEDGMENTS

We would like to thank anonymous referee for pointing out importance of energy losses of atomic nuclei and further useful comments and suggestions. The work of D. S. and A. N. has been supported in part by the French National Research Agency (ANR) Grant No. ANR-19-CE31-0020. Work of O. K. is supported in the framework of the State project “Science” by the Ministry of Science and Higher Education of the Russian Federation under Contract No. 075-15-2020-778.

-
- [1] R. U. Abbasi *et al.* (Telescope Array Collaboration), arXiv:2110.14827.
- [2] J. Kim, D. Ivanov, K. Kawata, H. Sagawa, and G. Thomson, *EPJ Web Conf.* **283**, 03005 (2023).
- [3] M. Kachelriess and D. V. Semikoz, *Astropart. Phys.* **26**, 10 (2006).
- [4] P. Abreu, M. Aglietta, E.J. Ahn, D. Allard, I. Allekotte, J. Allen, J. Alvarez Castillo, J. Alvarez-Muñiz, M. Ambrosio, and A. Aminaei (Pierre Auger Collaboration), *Astropart. Phys.* **34**, 314 (2010).
- [5] R. U. Abbasi *et al.* (Telescope Array Collaboration), *Astrophys. J. Lett.* **790**, L21 (2014).
- [6] P. Erdođdu, O. Lahav, J. P. Huchra, M. Colless, R. M. Cutri, E. Falco, T. George, T. Jarrett, D. H. Jones, L. M. Macri *et al.*, *Mon. Not. R. Astron. Soc.* **373**, 45 (2006).
- [7] H. Boehringer, G. Chon, and J. Truemper, *Astron. Astrophys.* **651**, A16 (2021).
- [8] A. Aab *et al.* (Pierre Auger Collaboration), *J. Cosmol. Astropart. Phys.* 04 (2017) 038; 03 (2018) E02.
- [9] A. Aab *et al.* (Pierre Auger Collaboration), *Phys. Rev. D* **96**, 122003 (2017).
- [10] K. Dolag, D. Grasso, V. Springel, and I. Tkachev, *JETP Lett.* **79**, 583 (2004).
- [11] S. Hackstein, F. Vazza, M. Brügggen, J. G. Sorce, and S. Gottlöber, *Mon. Not. R. Astron. Soc.* **475**, 2519 (2018).
- [12] K. Dolag, M. Kachelrieß, and D. V. Semikoz, *J. Cosmol. Astropart. Phys.* 01 (2009) 033.
- [13] R. Jansson and G. R. Farrar, *Astrophys. J.* **757**, 14 (2012).
- [14] M. S. Pshirkov, P. G. Tinyakov, and F. R. Urban, *Mon. Not. R. Astron. Soc.* **436**, 2326 (2013).
- [15] S. McAlpine, J. C. Helly, M. Schaller, T. Sawala, G. Lavaux, J. Jasche, C. S. Frenk, A. Jenkins, J. R. Lucey, and P. H. Johansson, *Mon. Not. R. Astron. Soc.* **512**, 5823 (2022). <https://github.com/okolo/uhecr-trace>.
- [16] R. Alves Batista, A. Dundovic, M. Erdmann, K.-H. Kampert, D. Kuempel, G. Müller, G. Sigl, A. van Vliet, D. Walz, and T. Winchen, *J. Cosmol. Astropart. Phys.* **05** (2016) 038.
- [17] M. S. Pshirkov, P. G. Tinyakov, P. P. Kronberg, and K. J. Newton-McGee, *Astrophys. J.* **738**, 192 (2011).
- [18] R. Jansson and G. R. Farrar, *Astrophys. J. Lett.* **761**, L11 (2012).
- [19] P. Terral and K. Ferrière, *Astron. Astrophys.* **600**, A29 (2017).
- [20] J. Kleimann, T. Schorlepp, L. Merten, and J. B. Tjus, *Astrophys. J.* **877**, 76 (2019).
- [21] R. Adam *et al.* (Planck Collaboration), *Astron. Astrophys.* **596**, A103 (2016).
- [22] G. Giacinti, M. Kachelrieß, and D. V. Semikoz, *Phys. Rev. D* **90**, 041302 (2014).
- [23] G. Giacinti, M. Kachelrieß, and D. V. Semikoz, *Phys. Rev. D* **91**, 083009 (2015).
- [24] G. Giacinti, M. Kachelriess, and D. V. Semikoz, *J. Cosmol. Astropart. Phys.* 07 (2018) 051.
- [25] T. R. Jaffe, *Galaxies* **7**, 52 (2019).
- [26] J. L. Han, R. N. Manchester, W. van Straten, and P. Demorest, *Astrophys. J. Suppl. Ser.* **234**, 11 (2018).
- [27] A. R. Taylor, J. M. Stil, and C. Sunstrum, *Astrophys. J.* **702**, 1230 (2009).
- [28] A. A. Abdo, M. Ackermann, M. Ajello, K. Asano, L. Baldini, J. Ballet, G. Barbiellini, D. Bastieri, B. M. Baughman, K. Bechtol *et al.*, *Astrophys. J.* **699**, 31 (2009).
- [29] A. Neronov, D. Semikoz, and I. Vovk, *Astron. Astrophys.* **519**, L6 (2010).
- [30] A. Neronov, P. Tinyakov, and I. Tkachev, *J. Exp. Theor. Phys.* **100**, 656 (2005).
- [31] H. Sagawa, *Proc. Sci. ICRC2015* (2016) 657.
- [32] A. Neronov and D. V. Semikoz, *Phys. Rev. D* **80**, 123012 (2009).
- [33] A. Neronov and I. Vovk, *Science* **328**, 73 (2010).
- [34] M. Ackermann *et al.* (Fermi-LAT Collaboration), *Astrophys. J. Suppl. Ser.* **237**, 32 (2018).
- [35] R. Banerjee and K. Jedamzik, *Phys. Rev. D* **70**, 123003 (2004).
- [36] M. S. Pshirkov, P. G. Tinyakov, and F. R. Urban, *Phys. Rev. Lett.* **116**, 191302 (2016).
- [37] A. Aramburo-Garcia, K. Bondarenko, A. Boyarsky, A. Neronov, A. Scaife, and A. Sokolenko, *Mon. Not. R. Astron. Soc.* **515**, 5673 (2022).
- [38] H. Katz, S. Martin-Alvarez, J. Rosdahl, T. Kimm, J. Blaizot, M. G. Haehnelt, L. Michel-Dansac, T. Garel, J. Oñorbe, J. Devriendt *et al.*, *Mon. Not. R. Astron. Soc.* **507**, 1254 (2021).
- [39] K. Jedamzik and A. Saveliev, *Phys. Rev. Lett.* **123**, 021301 (2019).

- [41] R. Durrer and A. Neronov, *Astron. Astrophys. Rev.* **21**, 62 (2013).
- [42] P. P. Kronberg, *Rep. Prog. Phys.* **57**, 325 (1994).
- [43] R. Plaga, *Nature (London)* **374**, 430 (1995).
- [44] A. Neronov and D. V. Semikoz, *JETP Lett.* **85**, 473 (2007).
- [45] I. Vovk, J. Biteau, H. Martínez-Huerta, M. Meyer, and S. Pita (CTA Consortium Collaboration), *Proc. Sci. ICRC2021 (2021)* 894.
- [46] A. Korochkin, O. Kalashev, A. Neronov, and D. Semikoz, *Astrophys. J.* **906**, 116 (2021).
- [47] D. Grasso and H. R. Rubinstein, *Phys. Rep.* **348**, 163 (2001).
- [48] L. M. Widrow, D. Ryu, D. R. G. Schleicher, K. Subramanian, C. G. Tsagas, and R. A. Treumann, *Space Sci. Rev.* **166**, 37 (2012).
- [49] S. Bertone, C. Vogt, and T. Enßlin, *Mon. Not. R. Astron. Soc.* **370**, 319 (2006).
- [50] F. Marinacci, M. Vogelsberger, R. Pakmor, P. Torrey, V. Springel, L. Hernquist, D. Nelson, R. Weinberger, A. Pillepich, J. Naiman *et al.*, *Mon. Not. R. Astron. Soc.* **480**, 5113 (2018).
- [51] A. A. Garcia, K. Bondarenko, A. Boyarsky, D. Nelson, A. Pillepich, and A. Sokolenko, *Mon. Not. R. Astron. Soc.* **505**, 5038 (2021).
- [52] K. Bondarenko, A. Boyarsky, A. Korochkin, A. Neronov, D. Semikoz, and A. Sokolenko, *Astron. Astrophys.* **660**, A80 (2022).
- [53] M. Sanati, Y. Revaz, J. Schober, K. E. Kunze, and P. Jablonka, *Astron. Astrophys.* **643**, A54 (2020).
- [54] P. A. R. Ade *et al.* (Planck Collaboration), *Astron. Astrophys.* **594**, A19 (2016).
- [55] P. Trivedi, K. Subramanian, and T. R. Seshadri, *Phys. Rev. D* **89**, 043523 (2014).
- [56] J. D. Bray and A. M. M. Scaife, *Astrophys. J.* **861**, 3 (2018).
- [57] A. Van Vliet, A. Palladino, A. Taylor, and W. Winter, *Mon. Not. R. Astron. Soc.* **510**, 1289 (2021).
- [58] A. Aab *et al.* (Pierre Auger Collaboration), *Astrophys. J. Lett.* **853**, L29 (2018).